Received: 23 January 2022 | Revised: 27 February 2022 | Accepted: 19 March 2022

DOI: 10.1111/ajt.17038

ORIGINAL ARTICLE

T cell depletion increases humoral response by favoring T follicular helper cells expansion

Rodrigo Benedetti Gassen[1] | Thiago J. Borges[1] | María José Pérez-Sáez[2,3] | Hengcheng Zhang[2] | Ayman Al Jurdi[1] | Laura Llinàs-Mallol[3] | Bruno Aoyama[2] | Maurício Lima[2] | Julio Pascual[3] | Peter T. Sage[2] | Naoka Murakami[2] | Leonardo V. Riella[1,4]

[1]Center of Transplantation Science, Department of Surgery, Massachusetts General Hospital, Harvard Medical School, Boston, Massachusetts, USA

[2]Renal Division, Brigham & Women's Hospital, Harvard Medical School, Boston, Massachusetts, USA

[3]Department of Nephrology, Hospital del Mar, Barcelona, Spain

[4]Department of Medicine, Division of Nephrology, Massachusetts General Hospital, Harvard Medical School, Boston, Massachusetts, MA, USA

Correspondence
Leonardo V. Riella, Center of Transplantation Science, Department of Surgery, Massachusetts General Hospital, Harvard Medical School, 149 13th St, Room 5102, Boston, Charlestown, MA 02129, USA.
Email: lriella@mgh.harvard.edu

Funding information
Assistant Secretary of Defense and Health Affairs, Grant/Award Number: W81XWH2010758; Post-doctoral fellowship grant from the American Heart Association (AHA); National Institute of Health (NIH) Grant R01, Grant/Award Number: AI143887

Antibody-mediated rejection is a major cause of long-term graft loss in kidney transplant patients. T follicular helper (Tfh) cells are crucial for assisting B cell differentiation and are required for an efficient antibody response. Anti-thymocyte globulin (ATG) is a widely used lymphocyte-depleting induction therapy. However, less is known about how ATG affects Tfh cell development and donor-specific antibody (DSA) formation. We observed an increase in circulating Tfh cells at 6 months after kidney transplant in patients who received ATG. Using an NP-OVA immunization model, we found that ATG-treated mice had a higher percentage of Tfh cells, germinal center B cells, and higher titers of antigen-specific antibodies compared to controls. ATG-treated animals had lower levels of IL-2, a known Bcl-6 repressor, but higher levels of IL-21, pSTAT3 and Bcl-6, favoring Tfh differentiation. In a mouse kidney transplant model, ATG-treated recipients showed an increase in Tfh cells, DSA and C4d staining in the allograft. Although ATG was effective in depleting T cells, it favored the expansion of Tfh cells following depletion. Concomitant use of IL-2, tacrolimus, or rapamycin with ATG was essential to control Tfh cell expansion. In summary, ATG depletion favors Tfh expansion, enhancing antibody-mediated response.

KEYWORDS
anti-thymocyte globulin, antibody-mediated rejection, DSA, follicular T helper cells, kidney transplantation, T cell depletion

1 | INTRODUCTION

Antibody-mediated rejection (ABMR) is a leading cause of long-term graft loss after kidney transplant recipients.[1,2] Although various immunosuppressive drugs have been tried as a treatment of ABMR, response rates have been poor, and more effective treatments are needed.[3] For an effective humoral response, T follicular helper (Tfh) cells, a $CD4^+$ T cell subset, are critical in providing help for germinal

Abbreviations: ABMR, antibody-mediated rejection; ATG, anti-thymocyte globulin; BSA, bovine serum albumin; CD, cluster of differentiation; CFA, complete Freund's adjuvant; CNI, calcineurin inhibitor; cTfh, circulating T follicular helper cells; DSA, donor-specific antibody; ELISA, enzyme-linked immunoassay; GC, germinal center; H&E, hematoxylin and eosin; HRP, horseradish peroxidase; Ig, immunoglobulin; IL, interleukin; LN, lymph node; MHC, major histocompatibility complex; NP, 4-hydroxy-3-nitrophenylacetyl; OVA, ovalbumin; PBMCs, peripheral blood mononuclear cells; PBS, phosphate buffered saline; PFA, paraformaldehyde; POD, post-operatory day; pSTAT, phosphorylated STAT; RAPA, rapamycin; SD, standard deviation; STAT, signal transducer and activator of transcription; TAC, tacrolimus; Tfh, T follicular helper cells; TMB, 3,3',5,5'-Tetramethylbenzidine.

center (GC) reactions which activate and differentiate B cells and produce high-affinity antibodies.[4] The percentage of circulating Tfh (cTfh) cells increases after kidney transplantation,[5] and it is even higher in transplanted patients with pre-existent DSA.[6] These findings suggest that Tfh cells play an important role in the pathophysiology of ABMR.

Anti-thymocyte globulin (ATG) is a mix of antibodies with multiple specificities directed against lymphocytes, both T and non-T cells.[7] Anti-thymocyte globulin is widely used in transplanted recipients as a lymphocyte-depleting induction therapy,[8] and different mechanisms including complement activation are responsible for the T cell depletion.[9,10] Upon T cell depletion, ATG promotes a homeostatic lymphopenia-induced proliferation of memory T cells and T regulatory cells.[11] Less is known about how ATG affects the different arms of the immune response, in particular, the humoral immune response, including Tfh cell development, B cell activation, and differentiation.

In the present study, we analyzed circulating Tfh cells in kidney transplant recipients that had received ATG and used two murine models to better understand the effect of ATG on Tfh cells, including (1) a murine kidney transplant model and (2) a mouse model with NP-OVA + CFA immunization, which allows tracking of antigen-specific response *in vivo*. We found that while murine ATG treatment was able to reduce total $CD4^+$ T cells in the blood and secondary lymphoid organs, it increased the percentages of antigen-specific Tfh cells and antibody-specific responses. Furthermore, we provided evidence that the low level of IL-2 and upregulation of circulating IL-21, pSTAT3, and Bcl-6 in T cells upon ATG treatment created a favorable microenvironment for the generation of Tfh cells. Combining ATG with recombinant IL-2, tacrolimus, or rapamycin was essential to control Tfh cell expansion and the generation of the humoral response.

2 | METHODS

2.1 | Peripheral blood mononuclear cells (PBMC) isolation

We used samples from a prospective study previously published.[12] Briefly, peripheral blood samples were obtained from patients before kidney transplant and 6 months after transplant. All samples were collected at the Lahey Clinic Medical Center, Burlington, MA, and processed in the Immunological Core Facility in the Transplant Research Center, Brigham and Women's Hospital. PBMCs were isolated using density-gradient centrifugation (Ficoll-Paque solution) (GE Healthcare Biosciences) and stored in liquid nitrogen.

2.2 | Mice

C57bl/6 and Balb/c mice were maintained as breeding colonies in the Harvard Medical School facility with water and food ad libitum. All mice used in the experiments were females between six to 10 weeks old. Animals were bred and housed in individual and standard mini-isolators under specific pathogen-free conditions. All animals were housed following the Institutional Animal Care and Use Committee (IACUC) and National Institutes of Health (NIH) Animal Care Guidelines.

2.3 | Murine ATG production

Murine ATG was generated as previously published.[13] Briefly, rabbit anti-mouse thymocyte serum was generated by the Hybridoma Core at the Cleveland Clinic Research Institute by immunizing rabbits with C3H, DBA1, and SJL thymocytes. Total IgG (murine ATG) was isolated with a sequential ammonium sulfate precipitation, followed by purification with Melon gel IgG Spin Purification Kit (ThermoScientific). Total protein concentration was measured using BCA assay (ThermoScientific), and the purity was confirmed with SDS-PAGE. The efficacy of murine ATG was checked by testing $CD4^+$ and $CD8^+$ T cell depletion in the spleen, lymph nodes (LNs), and peripheral blood in naïve mice.

2.4 | Immunization and treatments

C57bl/6 mice were immunized with 200 μg NP-OVA (Biosearch Technologies) emulsified in H37RA CFA subcutaneously in the flanks on day 0 and intraperitoneally treated with 500 μg of ATG or IgG control on day 0 and 4 post-immunization. At 6h, 48h, and day 8 after NP-OVA + CFA immunization, blood, spleen, and lymph nodes were collected for analysis. In some experiments, mice also received treatment with 250 μg of anti-CD4 (GK1.5 clone) every two days, or daily doses of 1 mg/kg of tacrolimus/ FK-506 (Sigma), 0.5 mg/kg of rapamycin (Sigma), or 30,000 U of recombinant mouse IL-2 (Biolegend).

2.5 | Kidney transplantation model

Kidney transplantations were performed as previously described in[14,15] in a sterile environment by qualified microsurgeons. The native kidneys of the recipient remained untouched as this was a non-life-sustaining approach. Following a midline abdominal incision, the left kidney, aorta, and inferior vena cava of the donor were exposed and mobilized. The kidney was procured en-bloc including the renal vein; the renal artery, along with a small aortic cuff; and the ureter. The vessels of the graft were anastomosed end-to-side to the recipient's abdominal aorta and inferior vena cava using 10-0 nylon sutures (AROSurgical, Newport Beach, CA). By using a pull-through, the ureter was directly anastomosed into the bladder. The time of cold ischemia of the graft was maintained at 40 min, and the warm ischemia was 30 min.

2.6 | Flow cytometry

Spleen, blood, and lymph nodes from C57bl/6 mice were collected and prepared for flow cytometry staining. Dead cells were excluded using the eBioscience Fixable Viability solution. An additional dump channel was used to exclude irrelevant cells using a mixture of antibodies (CD11c, F4/80, CD19, and CD3) depending on the staining panel. Additional antibodies for CD45, CD4, PD1, CXCR5, CD25, IL-21R, CD44, B220, CD40, CD38, IgD, IgG1, Fas, and GL7 were used to stain T and B cells populations. Incubation with the $OVA_{328-337}$-tetramer was performed at 37°C for 30 min before additional antibody staining. For the intracellular staining of Bcl-6, Blimp-1, T-bet, RORγT, Foxp3, and Gata-3, we used the eBioscience FOXP3 intracellular buffer following the manufacturer's instructions. All antibodies used were from Biolegend.

For pSTAT detection, cells were fixed with 1% PFA in PBS for 10 min at room temperature, permeabilized with True-Phos Perm Buffer (BioLegend) at −20°C, and stained with mouse anti-Stat5 (pY694, BD) and anti-Stat3 (pS727; BD) alongside surface-stain antibodies detailed above in permeabilization buffer (eBioscience). Samples were acquired using an LSRFortessa (BD) and analyzed using FlowJo (BD).

2.7 | Flow cytometry sorting and in vitro cocultures

After 7 days of NP-OVA + CFA immunization, spleen and draining lymph nodes from ATG or IgG-treated mice were harvested, and cells were incubated with Fc Block and fluorochrome-conjugated anti-CD3, anti-CD4, anti-CD19, anti-ICOS, and anti-CXCR5 for 30 min on ice. First, CD4 T cells ($CD3^+CD4^+CD19^-$) and B cells ($CD3^-CD4^-CD19^+$) were sorted and co-cultured in vitro in different combinations in an incubator at 37°C with 5% of CO_2. As a positive control, we used 2 μL/mL of anti-CD3 and 5 μL/mL of anti-IgM antibodies. After 6 days of incubation, the supernatant was stored for antibody quantification and cells were stained with anti-CD19, anti-MHCII, and anti-GL7 and analyzed with a flow cytometer. In some experiments, cells were sorted further as Tfh ($CD3^+CD4^+CXCR5^+ICOS^+CD19^-$) and non-Tfh ($CD3^+CD4^+CXCR5^-ICOS^-CD19^-$) cells.

2.8 | ELISA for NP, OVA-specific antibody, IL-2, IL-21, and donor specific antibody measurement

For NP or OVA-specific antibody ELISAs, Maxisorp plates were coated with 1 μg/mL of NP-BSA (Biosearch Technologies) or OVA (InvivoGen), followed by blocking for 1 h with BSA (5% BSA, 0.05% tween in PBS 1X buffer), and mice serum was added in a dilution of 1/5000 and incubated for 2 h at room temperature. Rabbit anti-mouse antibody HRP-conjugated (Invitrogen) and TMB (Life Technologies) were used for development. IL-2 and IL-21 concentrations in serum were determined by capturing ELISA (R&D Systems), according to the manufacturer's instructions. Plates were read on a plate reader (Spectramax).

For the donor specific-antibody measurement, we used Balb/c or C57bl/6 mice as probes for DSA quantification in the serum. 5×10^5 splenocytes were added to 96-well plates and after two washes, the cells were incubated for 30 min with serum from naïve, POD7, POD14, and POD20 of IgG-treated mice or ATG-treaded mice (1:40 dilution). Cells were then stained with Fixable viability Dye (eBioscience), anti-B220 (Biolegend), and anti-CD3 (Biolegend) in the presence of Fc-block (Biolegend). Cells were washed twice and incubated for 30 min with anti-IgG and anti-IgM (BDbioscience). Donor reactive antibody against MHC class II was measured by assessing anti-IgG or anti-IgM signal on total $B220^+$ cells and against MHC class I by assessing anti-IgG or anti-IgM signal on total $CD3^+$ cells by flow cytometry and expressed as mean fluorescence intensity (MFI).

2.9 | H&E and C4d staining

For H&E staining, kidneys were fixed with 10% formalin, embedded in paraffin and cut into 5 μm sections. Hematoxylin and eosin staining were performed by standard methods[16] to evaluate the cell infiltration.

Deposition of C4d in the kidney tissue was stained using a rat anti-mouse C4d antibody with a FITC-conjugated anti-rat secondary antibody. Briefly, frozen sections (8 μm) fixed with acetone were washed with PBS three times. The sections were blocked with PBS containing 1% bovine serum albumin (BSA) at room temperature for 1 h. The sections were stained by rat anti-mouse C4d antibody (clone 16D2, Novus Biologicals) diluted 1:100 with PBS containing 1% BSA, followed by FITC-conjugated anti-rat IgG antibody (Jackson ImmunoResearch) diluted 1:1000 for 1 h at room temperature. After washing 3 times with PBS, the fluorescent images were captured with a fluorescence microscope (Zeiss LSM 780).

2.10 | Statistical analysis

Data were tested for normality of distribution using a Kolmogorov–Smirnoff test. Differences between groups were analyzed with unpaired t-tests for two groups or a one-way ANOVA test for >2 groups followed by a Tukey correction for multiple pairwise comparisons. GraphPad Prism software (San Diego, CA) was used for statistical analysis. All tests were two-sided and an α level of 0.05 was considered significant. Values shown in graphs represent the mean ± standard deviation (SD).

3 | RESULTS

3.1 | Circulating Tfh cell percentages increase after kidney transplant in ATG-treated patients

To assess the kinetics of cTfh in kidney transplant patients who received induction therapy with ATG, we collected and analyzed PBMCs of these patients before and after transplantation

(Figure 1A). Briefly, this cohort was composed of kidney recipients with a mean age of 59 years old that received three doses (0.75 mg/Kg per dose) of rabbit ATG, 30% of the cohort were females, and the leading cause of kidney disease was diabetes. In addition, deceased donors represented 70% of the cohort, while all patients were non-sensitized (PRA of zero).[12] The demographics of the cohort are detailed in Table S1. Overall, we found an increase in cTfh cell ($CD4^+CXCR5^+PD\text{-}1^+$) percentages 6 months after transplantation compared with pre-transplantation (Figure 1B-C), although total $CD4^+$ T cells remained significantly depleted (Figure 1D).

3.2 | Increase in DSA and C4d staining generated by ATG in a kidney transplant model

We further assessed the capacity of ATG to modulate Tfh cells and alloantibody response in a non-survival-based model of kidney transplantation. BALB/c kidneys were transplanted into C57Bl/6 mice, and the recipients were treated with ATG (murine) or IgG control at post-operatory day (POD)0 and POD4 (Figure 1E). The flow cytometry gating strategy for Tfh and B cells can be seen in Figure S1. ATG treatment successfully decreased the percentages of $CD4^+$ T cells in the blood (Figure S2A). However, the percentage of cTfh cells were higher in the blood of ATG-treated mice at POD7 and POD20 compared to controls (Figure 1F), while no differences were seen in the absolute number of Tfh, total B cells, and GC B cells in the spleen at POD20 (Figure 1G-I). Nonetheless, the percentage and the absolute number of $IgG1^+$ B cells in the spleen (Figure 1J) and the serum levels of anti-MHC class I and class II DSAs (Figure 1K) were higher in the animals treated with ATG compared to IgG controls. To evaluate whether higher levels of DSAs were associated with greater alloantibody-mediated injury, we analyzed the kidney allografts for immune infiltration by H&E and antibody-allograft interaction with complement activation by C4d staining. We found tubulitis and interstitial inflammation in both ATG and IgG-treated mice but more significant microvascular inflammation (glomerulitis and peritubular capillaritis) in ATG-treated mice compared to controls (Figure 1L). We also found stronger C4d staining in peritubular capillaries in ATG-treated mice compared to IgG-treated mice (Figure 1M). Taken together, these data indicate that ATG treatment alone is associated with increased generation of an early alloantibody response and antibody-mediated allograft injury in a kidney transplantation model.

3.3 | Antigen-specific Tfh cells were enriched in LNs after ATG treatment

To better understand the impact of ATG on Tfh cells, we used a murine model of NP-OVA immunization and analyzed whether ATG could modulate the formation of Tfh cells. C57Bl/6 mice were immunized with NP-OVA + CFA at day 0 and treated with murine ATG or IgG control at days 0 and 4. On day 8 after immunization, cells from peripheral blood and secondary lymphoid organs were analyzed (Figure 2A). ATG-treated animals had lower percentage and absolute numbers of $CD4^+$ T cells in the draining lymph nodes (Figure 2B-C), blood, and spleen (Figure S2B). When we analyzed the Tfh cell ($CD4^+CXCR5^+PD\text{-}1^+$) compartment, the percentages and absolute numbers were increased in the ATG-treated group compared with the IgG control group (Figure 2D-E). In addition, the proportion of OVA-specific $CD4^+$ Tfh cells was higher in ATG-treated animals, but ATG treatment did not affect the percentage of OVA-specific non-Tfh cells compared to IgG treatment (Figure 2F).

3.4 | ATG increased antigen-specific humoral response

Based on the expansion of Tfh cells, we next tested the effect of ATG on GC formation and antigen-specific antibody production after NP-OVA immunization. On day 8 after immunization, the percentage of total B cells (Figure 3A-B), GC B cells (Figure 3C-D), and class-switched $IgG1^+$ B cells (Figure 3E-F) in the draining lymph nodes were higher in the ATG-treated group compared to IgG-treated control group. In blood and spleen, the action of ATG was similar to the lymph nodes (data not shown).

To prove that the increase of Tfh and B cells by ATG might induce specific antibody production, and this activation was dependent on $CD4^+$ T cells, we depleted $CD4^+$ T cells using a murine anti-CD4 monoclonal antibody in our model of NP-OVA immunization and analyzed the amount of specific IgG in serum by ELISA. On day 8, NP-specific (Figure 3G) and OVA-specific (Figure 3H) serum IgG were increased in ATG-treated mice. However, no detectable IgG was found in the absence of $CD4^+$ T cells. These results highlight the capacity of ATG to induce an antigen-specific humoral response in a $CD4^+$ T cell-dependent manner.

3.5 | Total $CD4^+$ T cells from ATG-treated mice have greater capacity in enhancing B cell response

To determine the capacity of $CD4^+$ T cells from ATG-treated mice to increase humoral immune responses, we used an in vitro CD4-mediated B cell stimulation assay.[15,17] Briefly, animals were immunized with NP-OVA + CFA with or without ATG treatment, and after 8 days, total B cells (gated as $CD3^-$ $CD19^+$), $CD4^+$ T cells (gated as $CD3^+CD4^+CD19^-$), or Tfh cells (gated as $CD3^+CD4^+ICOS^+CXCR5^+$ $CD19^-$) were sorted from the spleen of ATG- or IgG-treated mice. Cells were co-cultured for 6 days with anti-CD3 and IgM stimulations. B cells in the presence of either $CD4^+$ T cells from ATG or IgG-treated mice increased the frequency of $IgG1^+GL7^+$ GC B cells. However, we saw enhanced B cell differentiation to class-switched B cells, when B cells were co-cultured in the presence of

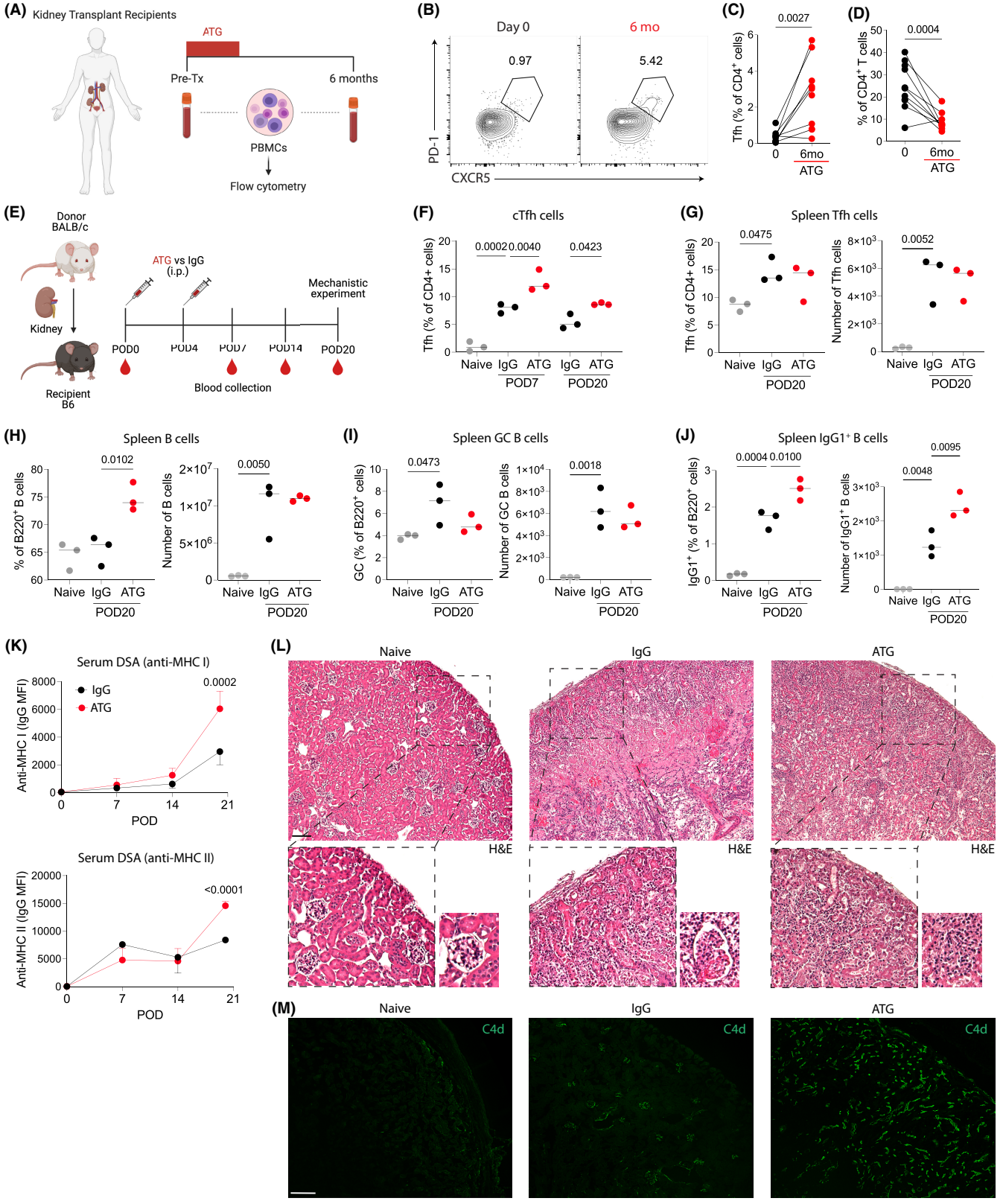

CD4+ T cells from ATG-treated mice (Figure 4A-B). Similarly, there was greater evidence of IgG1 generation in the co-cultures with ATG-treated CD4+ T cells (Figure 4C). In contrast, the B cell helper capacity in the presence of Tfh cells from ATG or IgG-treated mice showed no difference (Figure 4D-F). Together, these data demonstrate that ATG expanded the proportion of Tfh cells in the pool of total CD4+ T cells but did not increase the helper capacity of Tfh cells on a per-cell basis.

3.6 | Tacrolimus or rapamycin combination with ATG blocked the humoral response induced by ATG

Based on the low incidence of early antibody-mediated rejection post-transplant in ATG-treated kidney patients, we hypothesized that additional immunosuppression agents may contribute to mitigating Tfh cell expansion and B cell activation upon ATG treatment. To test this, we used the same NP-OVA model as depicted in Figure 1D, but mice were now treated with ATG in combination with either tacrolimus or rapamycin. Serum and lymph nodes were analyzed at day 8 post-immunization (Figure 5A). We found that the ATG in combination with tacrolimus or rapamycin was able to decrease the total $CD4^+$ T cells percentages and absolute numbers compared with the group treated only with ATG (data not shown). Moreover, both combinations successfully decreased the absolute numbers of Tfh cells (Figure 5B-C), GC B (Figure 5D-E), $IgG1^+$ B cells (Figure 5F-G), and NP- and OVA-specific antibodies (Figure 5H-I). Therefore, ATG must be combined with other immunosuppressive drugs to prevent Tfh cell expansion and the generation of the humoral response.

3.7 | IL-2 deficiency upon T cell depletion with ATG drives Tfh differentiation

To investigate the capacity of ATG to induce Tfh cell expansion, we evaluate the signals needed to induce the differentiation of Tfh cells. We first evaluate the capacity of ATG to induce the differentiation of other $CD4^+$ T cells subsets besides Tfh cells. ATG-treated mice also had an increase in the proportion of regulatory T cells while no significant changes were observed in Th1, Th2, or Th7 phenotypes compared with control mice (Figure 6A). In addition, ATG increased serum levels of IL-21 at 48 hours after immunization with NP-OVA (Figure 6B). On the other hand, the Bcl-6 repressor cytokine IL-2 was decreased in the serum 6 hours after immunization with NP-OVA in ATG-treated mice (Figure 6C). This suggests that less IL-2 availability caused by ATG induced T cell depletion creates a favorable environment for Tfh differentiation (Figure 6D). To test this hypothesis, we restore IL-2 levels in NP-OVA immunized and ATG-treated mice by treating the animals with i.p. injections of 30 000 U of recombinant murine IL-2 twice a day for 8 days (Figure 6E). ATG treatment was associated with an increase in the expression of pSTAT3 (Figure 6F) and the transcription factor Bcl-6 (Figure 6G) on $CD4^+$ T cells from draining lymph nodes. The restoration of IL-2 in ATG-treated mice decrease Bcl-6 (Figure 6G) expression but not pSTAT3 (Figure 6F) on $CD4^+$ T cells. In contrast to ATG-treated animals, ATG + IL-2 treatments induced pSTAT5 (Figure 6H) and Blimp-1 (Figure 6I) upregulation on $CD4^+$ T cells in draining lymph nodes. The combination of ATG + IL-2 was also able to control the enhancement of Tfh cells (Figure 6J), GC B cells (Figure 6L), $IgG1^+$B cells (Figure 6M), and NP-specific antibody production (Figure 6N). Taken together, the low levels of IL-2 induced by ATG treatment were able to activate pathways responsible to promoted Tfh cells differentiation and antibody production. The restoration of IL-2 in the microenvironment block ATG-induced humoral response.

4 | DISCUSSION

Antibody-mediated rejection is a major cause of graft loss and T follicular cells play an essential role in the generation of an antigen-specific antibody response. In the present study, we demonstrated that anti-thymoglobulin (ATG) induction leads to an expansion of Tfh cells and enhances humoral response in the absence of additional immunosuppressive drugs. We used two in vivo models (NP-OVA immunization and a kidney transplant model) to assess Tfh cells, B cell maturation, and antigen-specific antibody generation. Furthermore, we identified that T cell depletion by ATG created a favorable environment for Tfh cell expansion with low IL-2 levels and high IL-21. Thus, our data demonstrate that ATG treatment favors antigen-specific Tfh expansion, enhancing antibody-mediated response.

Rabbit ATG is used as induction therapy in over 70% of all kidney transplants performed in the United States.[18] It is the most common T cell depletion agent used in the clinic, though some transplant centers use alemtuzumab, an anti-CD52 monoclonal antibody, as an alternative. ATG induces a fast and sustained T cell depletion in the circulation and secondary lymphoid tissues by targeting a combination of T cell antigens, inducing complement-mediated cell death. Under lymphopenic conditions, remaining T cells undergo substantial homeostatic expansion.[19] The expanding lymphocytes have a dominant memory phenotype, and this homeostatic proliferation has been proposed as a major barrier to the induction of transplant tolerance.[20,21] Our study further contributes to this finding by indicating that during homeostatic proliferation, T follicular helper cells are preferentially expanded,

FIGURE 1 ATG treatment increases the proportion of Tfh cells in kidney transplant recipients and the alloantibody response in a mouse kidney transplant model. (A) PBMCs from kidney transplant recipients before and 6 months after kidney transplantation were isolated and characterized by flow cytometry. (B) Representative flow cytometry contour plots, (C) the frequency of circulating Tfh ($CD4^+CXCR5^+PD\text{-}1^+$) cells, and (D) total $CD4^+$ T cells (data from 10 patients; Wilcoxon matched-pairs signed-rank test). (E) BALB/c donor kidneys were transplanted into C57Bl/6 recipients, and the recipients were intraperitoneally treated with 500 μg of murine ATG or IgG control at POD0 and POD4. Mice were euthanized at POD20 after immunization, and blood, graft, and spleens were analyzed. Naïve mice were used as additional controls. (F) The frequency of circulating Tfh cells at POD7 and POD20. The frequency and absolute cell number of (G) Tfh cells, (H) total B cells, (I) GC B cells, and (J) $IgG1^+$ B cells at POD20 in the spleen. (K) Anti-MHC I and anti-MHC II DSA quantification in the serum over time post-transplantation. (L) Representative H&E and (M) C4d staining in the grafts at POD20. Scale bar, 100 μm. (E-M) Data as mean ± SD are shown ($n = 3$ per group; statistic by one-way ANOVA with Tukey multiple comparisons test)

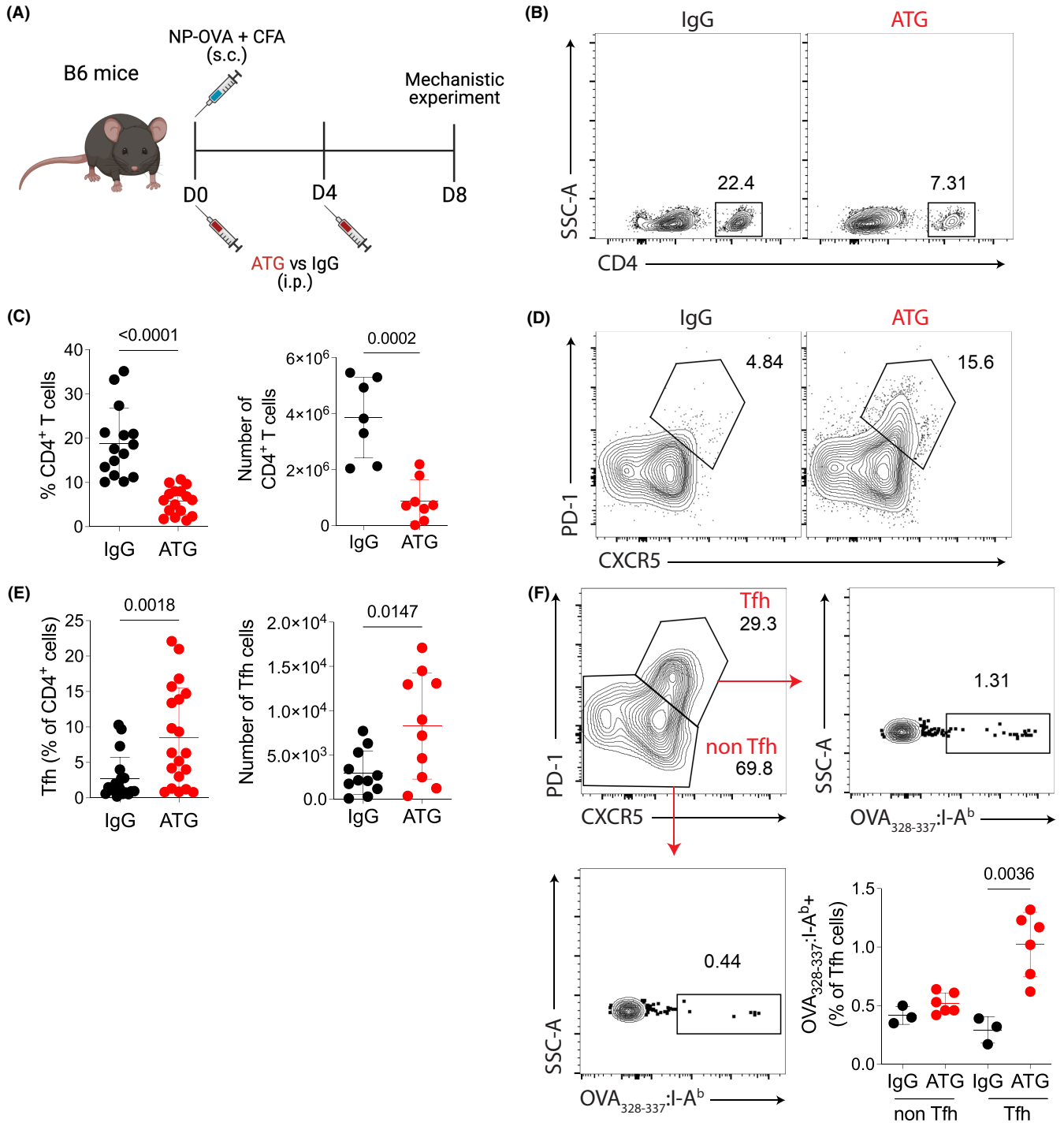

FIGURE 2 ATG treatment induces antigen-specific Tfh cells expansion. (A) C57Bl/6 mice were subcutaneously immunized with NP-OVA + CFA and intraperitoneally treated with 500 µg of murine ATG or IgG control on days 0 and 4. On day 8 after immunization, lymph nodes were analyzed by flow cytometry. (B) Representative flow cytometry contour plots of $CD4^+$ T cells in lymph nodes gated in Dump-live cells. (C) The frequency and absolute cell numbers per lymph node of total $CD4^+$ T cells. (D) Representative flow cytometry contour plots of Tfh ($CD4^+CXCR5^+PD\text{-}1^+$) cells in lymph nodes. (E) The frequency and absolute cell number per lymph node of Tfh ($CD4^+CXCR5^+PD\text{-}1^+$) cells. (F) Representative contour plots of and frequency of $OVA_{323\text{-}339}$-tetramer$^+$ cells in Tfh ($CD4^+CXCR5^+PD\text{-}1^+$) and non-Tfh ($CD4^+CXCR5^-PD\text{-}1^-$) cells. (A-F) Red dots represent the ATG-treated mice, and the black dots represent the IgG-treated mice. Data as mean ± SD are shown (pooled data from three independent experiments, with $n = 5$ per group; *t*-test). (C and E) Statistic by *t*-test. (F) Statistic by two-way ANOVA with Tukey multiple comparisons test

with the potential to promote humoral response. Indeed, the severe T cell depletion by alemtuzumab has been associated with a higher risk of antibody-mediated rejection in particular when drug minimization was attempted post-transplant.[22,23] Clinical trials comparing rabbit ATG and non-depleting induction therapies showed the benefit of ATG induction in sensitized patients.[24,25]

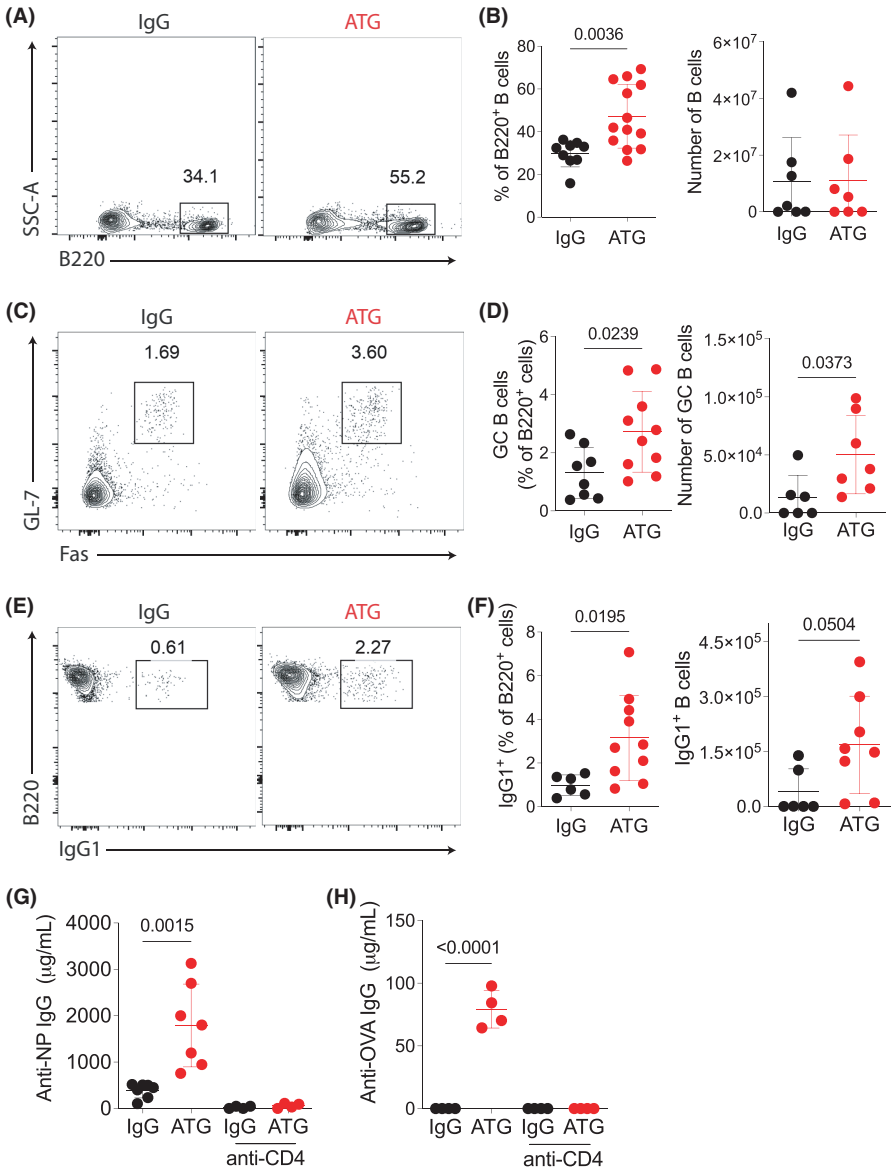

FIGURE 3 ATG treatment enhances antibody-specific immune response. C57Bl/6 mice were subcutaneously immunized with NP-OVA + CFA and intraperitoneally treated with 500 µg of murine ATG or IgG control. Mice were euthanized on day 8 after immunization, lymph nodes were analyzed by flow cytometry, as shown in Figure 2A. (A) Representative contour plots of $B220^+$ B cells in lymph nodes gated in Dump-live cells. (B) The frequency and absolute cell number of $B220^+$ B cells in lymph nodes. (C) Representative contour plots of GC B ($B220^+GL\text{-}7^+Fas^+$) cells in lymph nodes gated in $B220^+$ cells. (D) The frequency and absolute cell number per lymph node of GC B cells. (E) Representative contour plots of $B220^+$ $IgG1^+$ cells in lymph nodes gated in $B220^+$ cells. (F) The frequency and absolute cell number per lymph node of $IgG1^+$ B cells. (G) ELISA quantification of serum NP-specific IgG antibodies and (H) OVA-specific IgG antibodies at day 8 after immunization in controls or ATG-treated mice with subsequent selective depletion of CD4 cells (anti-CD4 depleting antibody). (A-H) Red dots represent the ATG-treated mice, and the black dots represent the IgG-treated mice. Data as mean ± SD are shown (pooled data from three independent experiments, with $n = 4–5$ per group). (B, D, and F) Statistic by *t*-test. (G-H) Statistic by two-way ANOVA with Tukey multiple comparisons test

Therefore, we think that concurrent adequate maintenance immunosuppression in the early post-transplant period is key to arresting this Tfh expansion irrespective of lymphocyte count. Furthermore, withdrawing CNI at 6 months post-transplant in low immunological risk patients that received ATG induction may also be associated with de novo DSA generation in up to 42% of patients, as it has been shown by Hricik et al. in the CTOT-9 trial.[26] Delaying initiation, dose minimization, or withdrawal of calcineurin inhibitors may favor the development of an antibody-mediated alloimmune response.

High-affinity antibodies result from the contact between Tfh cells and B cells in germinal centers, and this interaction has recently been implicated as fundamental to modulate antibody-mediated rejection.[27] We observed an increase in the percentages of cTfh cells at 6 months after transplant in kidney transplant patients that received ATG as an induction even though maintenance

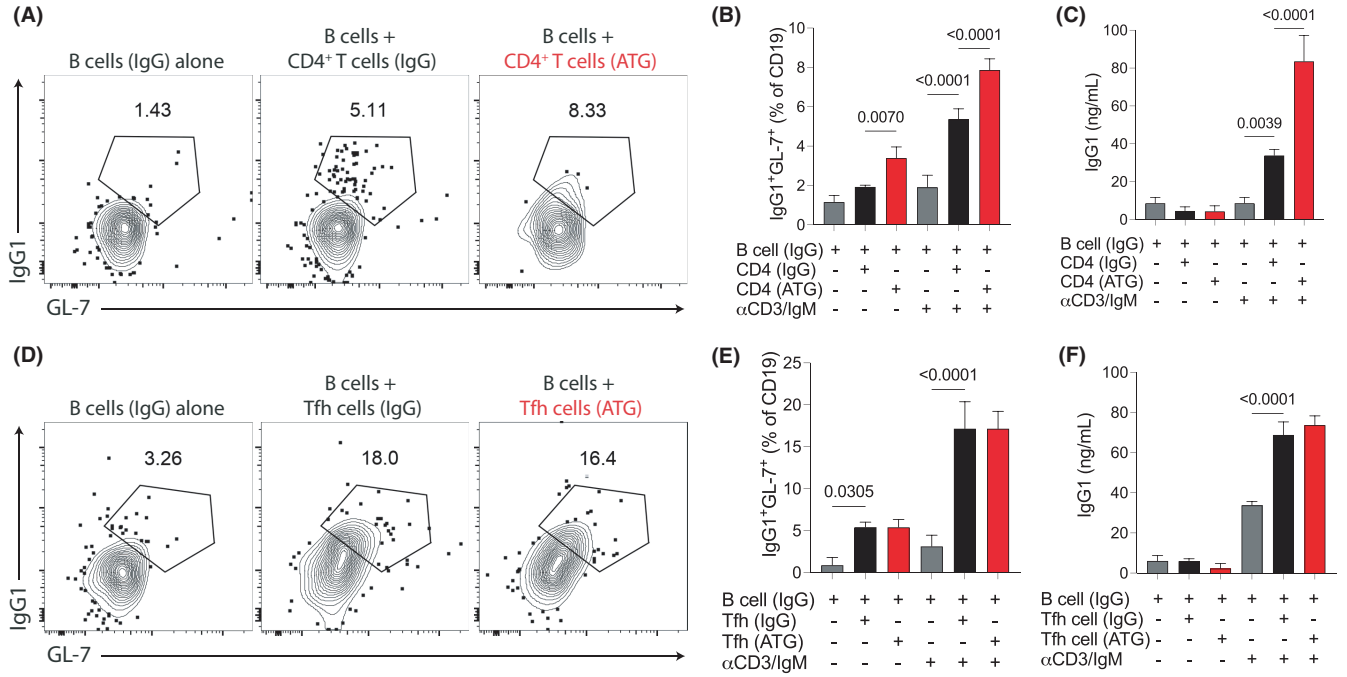

FIGURE 4 Total CD4$^+$ T cells from ATG-treated mice have an increased capacity to induce help to B cells in vitro. C57Bl/6 mice were subcutaneously immunized with NP-OVA + CFA and treated with 500 μg of murine ATG or IgG control. Mice were sacrificed at day 8 after immunization, and B cells, total CD4$^+$ T cells, or Tfh cells were sorted from the spleen and cocultured in vitro for 6 days in the presence or not of anti-CD3 and anti-IgM stimulation. (A) Representative contour plots and (B) frequency of IgG1$^+$ GC B cells (B220$^+$GL-7$^+$IgG1$^+$) in B cells cultured with total CD4$^+$ T cells. The IgG1$^+$ GC B cells are gated on CD19$^+$ MHCII$^+$ cells. (C) ELISA quantification of IgG1 antibodies in the supernatant of total CD4$^+$ T cells cultured with B cells. (D) Representative contour plots and (E) frequency of IgG1$^+$ GC B cells (B220$^+$GL-7$^+$IgG1$^+$) in B cells cultured with total Tfh cells. The IgG1$^+$ GC B cells are gated on CD19$^+$ MHCII$^+$ cells. (F) ELISA quantification of IgG1 antibodies in the supernatant of Tfh cells cultured with B cells. (A-F) All the B cells were from IgG-treated animals. Gray bars represent B cells alone, the black bars represent B cells coculture with CD4$^+$ T cells or Tfh cells from IgG-treated mice, and the red bars represent B cells coculture with CD4$^+$ T cells or Tfh cells from ATG-treated mice. Data as mean ± SD are shown (pooled data from three independent experiments; one-way ANOVA with Tukey multiple comparisons test)

therapy was started at post operatory day 1. Similar to our findings, Tfh cell activation in ATG-treated patients was also found by Macedo et al. In their study, they compared 31 kidney transplant patients that received ATG with 20 kidney transplant patients that received basiliximab for induction therapy.[28] ATG treated-patients showed upregulation of PD-1, and an activated and highly proliferative profile of Th1-like cTfh cells. Moreover, the percentage of effector memory cTfh cells and serum IL-21 in DSA$^+$ patients was significantly higher than those of stable patients in the ATG group.[28] In face of the deleterious effect of the DSA in kidney allograft survival,[2930] it is crucial to control the expansion of Tfh cells with the right dose and timing of other immunosuppressive drugs such as tacrolimus to prevent DSA formation.

We propose that ATG modify the immune environment by favoring the pathways responsible for inducing Tfh cell development. The phosphorylation of STAT3, the transcriptor factor Bcl6, and the cytokine IL-21 have broad effects on Tfh cell biology and provide insight into how regulation of these signals mediates naïve CD4$^+$ T cells differentiation into Tfh cells.[31-33] Bcl6 and pSTAT3 expression were increased in ATG-treated mice, and this was reflected in the amount of IL-21 in the serum. Higher IL-21 levels in the serum using a T cell-depleting agent (alemtuzumab) was also observed by Jones et al.[34] Although the authors did not focus in the antibody response, they showed secondary autoimmunity following alemtuzumab treatment of multiple sclerosis patients and higher T cells apoptosis driven by an increase in IL-21.[34]

Another important factor that interferes with Tfh differentiation is the cytokine IL-2. IL-2 is known to induce the expression of the transcription factor Blimp-1, responsible for controlling the terminal differentiation of B cells into antibody-secreting plasma cells. However, Blimp1 represses the expression of Bcl6.[35] The balance between Blimp-1 and Bcl6 expression is thought to control the relative commitment of CD4$^+$ T cells into the Tfh pathways.[36,37] In addition to Blimp-1, the phosphorylation of STAT5, which is potently activated by IL-2, antagonizes this process preventing Tfh cell differentiation and favoring the differentiation of other CD4$^+$ T cell subsets.[38] Since the primary source of IL-2 comes from T cells,[39] we observed depletion in IL-2 when we evaluated its levels in the serum after NP-OVA immunization and the first dose of ATG. Along those lines, recombinant IL-2 was demonstrated to inhibit Tfh responses and antibody production against influenza in the absence of T regulatory cells.[38] Moreover, low doses of IL-2 are also known to induce

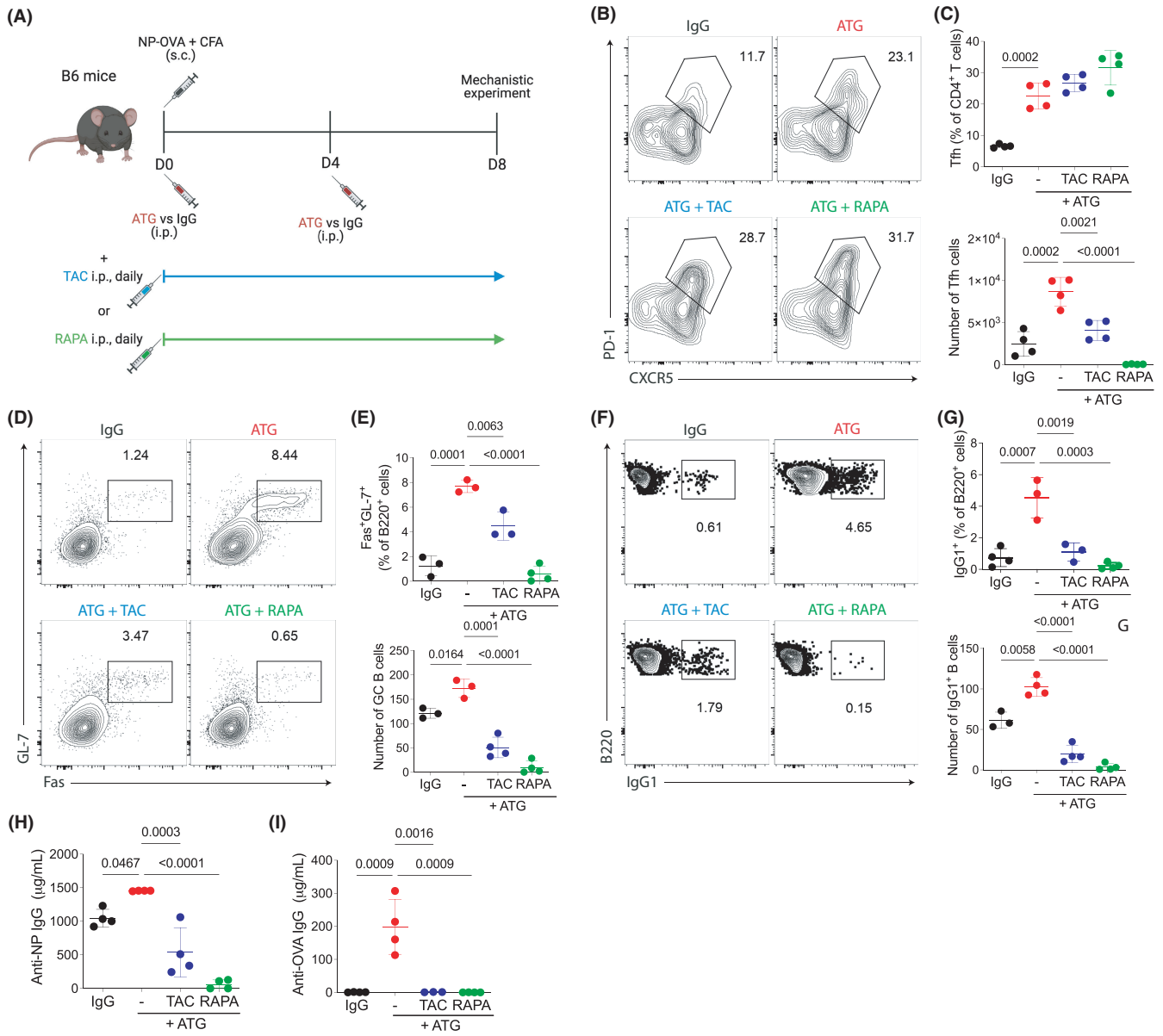

FIGURE 5 ATG combinations with tacrolimus or rapamycin control humoral response induced by ATG treatment alone. (A) C57Bl/6 mice were subcutaneously immunized with NP-OVA + CFA and treated with 500 µg of murine ATG or IgG control. A subgroup then received either 1 mg/Kg of tacrolimus or 0.5 mg/Kg of rapamycin, intraperitoneally, daily. Mice were euthanized at day 8 after immunization, and serum and lymph nodes were analyzed, as shown in Figure 2A. (B) Representative contour plots of Tfh ($CD4^+CXCR5^+$ $PD\text{-}1^+$) cells in lymph nodes gated in $CD4^+$ cells. (C) The frequency and absolute cell number per lymph node of Tfh cells. (D) Representative contour plots of GC B ($B220^+GL\text{-}7^+$ Fas^+) cells in lymph nodes gated in $B220^+$ cells. (E) The frequency and absolute cell number per lymph node of GC B cells. (F) Representative contour plots of $B220^+$ $IgG1^+$ cells in lymph nodes gated in $B220^+$ cells. (G) The frequency and absolute cell number per lymph node of $IgG1^+$ B cells. ELISA quantification of serum (H) NP-specific and (I) OVA-Specific IgG antibodies at day 8 after immunization. (A-I) Red dots represent the ATG-treated mice, black dots represent the IgG-treated mice, blue dots represent the ATG + tacrolimus-treated mice, and green dots represent the ATG + rapamycin-treated mice. Data as mean ± SD are shown (data from three independent experiments; with $n = 4$ per group; one-way ANOVA with Tukey multiple comparisons test)

T regulatory cells in mouse models and can be used as a treatment to control graft rejection[40] and autoimmune diseases.[41] In our model, in addition to Tfh cells enrichment, we observed an expansion of the T regulatory phenotype but no increase in T follicular regulatory cells (Figure S2C). These data align with studies that indicated that $CD4^+$ T cells subsets might have different ATG-susceptibilities.[42] Finally, we found that restoring IL-2 levels in ATG-treated mice blocked the signals required in Tfh differentiation by inducing pSTAT5 and Blimp-1.

In conclusion, we are not questioning the benefits of T cell depletion by ATG as it has clearly been shown as an effective induction therapy in high-risk patients when used in combination with other immunosuppressive drugs for the prevention of acute rejection.[43] However, understanding the mechanisms of action of immunosuppressive drugs

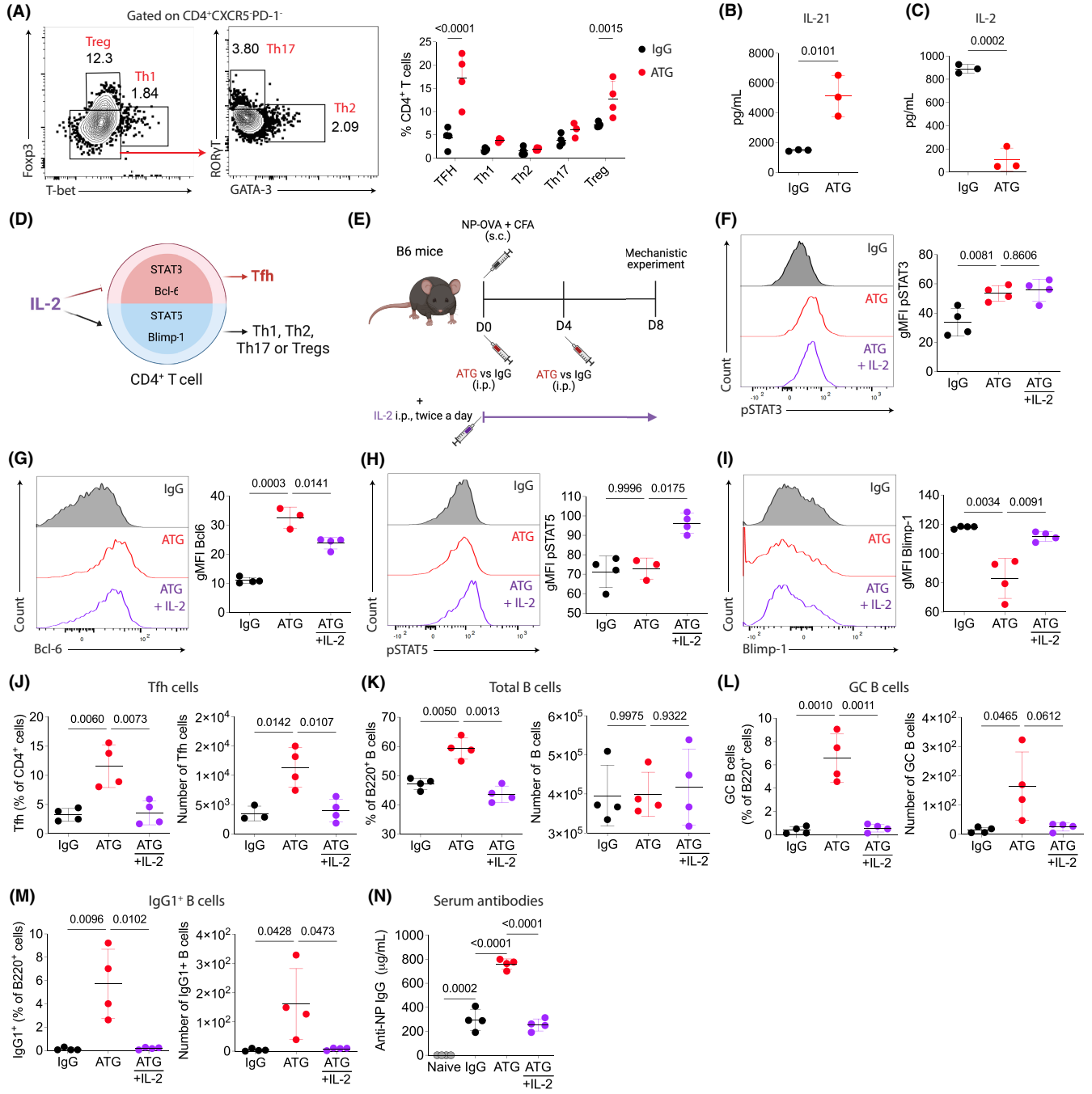

FIGURE 6 IL-2 signaling inhibits ATG-mediated humoral response. Using the NP-OVA + CFA immunization with either IgG or ATG treatment as shown in Figure 1D, we determined (A) the frequency of Tfh ($CD4^+CXCR5^+PD\text{-}1^+$), Th1 ($CD4^+CXCR5^-PD\text{-}1^-FOXP3^-Tbet^+$), Th2 ($CD4^+CXCR5^-PD\text{-}1^-FOXP3^-Tbet^-Gata3^+$), Th17 ($CD4^+CXCR5^-PD\text{-}1^-FOXP3^-Tbet^-RORγT^+$), and Treg ($CD4^+CXCR5^-$ $PD\text{-}1^-FOXP3^+$ $Tbet^-$) cells at day 8 after NP-OVA + CFA immunization in lymph nodes, (B) serum IL-21 levels after 48 h of immunization with NP-OVA + CFA, and the (C) serum IL-2 levels after 6 h of immunization with NP-OVA + CFA with IgG or ATG treatment. (D) Cartoon of the IL-2 signaling pathway in $CD4^+$ T cell differentiation. (E) C57Bl/6 mice were subcutaneously immunized with NP-OVA + CFA and treated with 500 μg of murine ATG or IgG control. A subgroup then received ATG and 30,000 U of recombinant mouse IL-2, intraperitoneally, twice a day. Mice were euthanized at day 8 after immunization, and serum and lymph nodes were analyzed, as shown in Figure 2A. Quantification of the geometric mean fluorescence intensity (gMFI) of (F) pSTAT3, (G) Bcl6, (H) pSTAT5, and (I) Blimp-1 in $CD4^+$ T cells from draining lymph nodes. Red histograms and red dots represent the ATG-treated mice, black histogram and dots represent the IgG-treated mice, and the purple histograms and dots represent the ATG-treated mice that received IL-2. The frequency and absolute cell number of (J) Tfh cells, (K) total B cells, (L) GC B cells, and (M) $IgG1^+$ B cells in the draining lymph node. (N) ELISA quantification of serum NP-specific IgG antibodies at day 8 after immunization. Naïve mice were used as additional controls. Data as mean ± SD are shown ($n = 4$ per group; one-way ANOVA with Tukey multiple comparisons test)

is essential to find the best combinations and timing to maximize the suppression of effector T cells and reduce the risk of infection, side effects, and alloantibody responses. Furthermore, measuring circulating Tfh cell numbers, IL-2, and IL-21 in addition to the current standard of measuring circulating anti-HLA antibodies in the serum could be a potential marker of patients at higher risk of antibody-mediated rejection. Based on our data, delaying CNI initiation after ATG induction in patients with delayed graft function may lead to deleterious effects by favoring the development of Tfh cells and potentially promoting alloantibody generation.

ACKNOWLEDGMENTS

This work was in part supported by the following research grants: National Institute of Health (NIH) Grant R01 AI143887 (to L.V.R.), the Assistant Secretary of Defense and Health Affairs, through the Reconstructive Transplant Research (RTR), under Award No. W81XWH2010758 and W81XWH2110904 (to L.V.R.). Opinions, interpretations, conclusions, and recommendations are those of the author and are not necessarily endorsed by the Department of Defense; T.J.B. is a recipient of a post-doctoral fellowship grant from the American Heart Association (AHA). This study was in part supported by the Harold and Ellen Danser Endowed Chair in Transplantation at Massachusetts General Hospital (Boston, MA, USA). Cartoons were created with BioRender.com.

DISCLOSURE

The authors of this manuscript have no conflicts of interest to disclose as described by the *American Journal of Transplantation*.

DATA AVAILABILITY STATEMENT

The data that support the findings of this study are available from the corresponding author upon reasonable request.

ORCID

María José Pérez-Sáez https://orcid.org/0000-0002-8601-2699
Hengcheng Zhang https://orcid.org/0000-0002-2562-1247
Laura Llinàs-Mallol https://orcid.org/0000-0003-4696-3331
Julio Pascual https://orcid.org/0000-0002-4735-7838
Peter T. Sage https://orcid.org/0000-0002-7287-0326
Naoka Murakami https://orcid.org/0000-0001-8168-5811
Leonardo V. Riella https://orcid.org/0000-0002-7636-3196

REFERENCES

1. Halloran PF, Chang J, Famulski K, et al. Disappearance of T cell-mediated rejection despite continued antibody-mediated rejection in late kidney transplant recipients. *J Am Soc Nephrol*. 2015;26:1711-1720.
2. Sellarés J, de Freitas DG, Mengel M, et al. Understanding the causes of kidney transplant failure: The dominant role of antibody-mediated rejection and nonadherence. *Am J Transplant*. 2012;12:388-399.
3. Böhmig GA, Eskandary F, Doberer K, Halloran PF. The therapeutic challenge of late antibody-mediated kidney allograft rejection. *Transpl Int*. 2019;32:775-788.
4. Sage PT, Sharpe AH. T follicular regulatory cells in the regulation of B cell responses. *Trends Immunol*. 2015;36(7):410-418. 10.1016/j.it.2015.05.005
5. Cano-Romero FL, Goya RL, Utrero-Rico A, et al. Longitudinal profile of circulating T follicular helper lymphocytes parallels anti-HLA sensitization in renal transplant recipients. *Am J Transplant*. 2019;19:89-97.
6. de Graav GN, Dieterich M, Hesselink DA, et al. Follicular T helper cells and humoral reactivity in kidney transplant patients. *Clin Exp Immunol*. 2015;180:329-340.
7. Bamoulid J, Crépin T, Courivaud C, et al. Antithymocyte globulins in renal transplantation—from lymphocyte depletion to lymphocyte activation: The doubled-edged sword. *Transplant Rev*. 2017;31:180-187.
8. Mohty M, Bacigalupo A, Saliba F, et al. New directions for rabbit antithymocyte globulin (thymoglobulin ®) in solid organ transplants, stem cell transplants and autoimmunity. *Drugs*. 2014;74:1605-1634.
9. Haudebourg T, Poirier N, Vanhove B. Depleting T-cell subpopulations in organ transplantation. *Transpl Int*. 2009;22:509-518.
10. Genestier L, Fournel S, Flacher M, et al. Induction of fas (Apo-1, CD95)-mediated apoptosis of activated lymphocytes by polyclonal antithymocyte globulins. *Blood*. 1998;91:2360-2368.
11. Lopez M, Clarkson MR, Albin M, Sayegh MH, Najafian N. A novel mechanism of action for anti-thymocyte globulin: Induction of CD4+CD25+Foxp3+ regulatory T cells. *J Am Soc Nephrol*. 2006;17:2844-2853.
12. Grafals M, Smith B, Murakami N, et al. Immunophenotyping and efficacy of low dose ATG in non-sensitized kidney recipients undergoing early steroid withdrawal: A randomized pilot study. *PLoS One*. 2014;9:e104408.
13. Ayasoufi K, Fan R, Fairchild RL, Valujskikh A. CD4 T cell help via B cells is required for lymphopenia-induced CD8 T cell proliferation. *J Immunol*. 2016;196:3180-3190.
14. Lei Y, Ehle B, Kumar SV, et al. Cathepsin S and protease-activated receptor-2 drive alloimmunity and immune regulation in kidney allograft rejection. *Front Cell Dev Biol*. 2020;8:1-12.
15. Mohammed MT, Cai S, Hanson BL, et al. Follicular T cells mediate donor-specific antibody and rejection after solid organ transplantation. *Am J Transplant*. 2021;21:1893-1901.
16. Chen J, Chen JK, Conway EM, Harris RC. Survivin mediates renal proximal tubule recovery from AKI. *J Am Soc Nephrol*. 2013;24:2023-2033.
17. Clement RL, Daccache J, Mohammed MT, et al. Follicular regulatory T cells control humoral and allergic immunity by restraining early B cell responses. *Nat Immunol*. 2019;20:1360-1371.
18. Hart A, Lentine KL, Smith JM, et al. OPTN/SRTR 2019 annual data report: Kidney. *Am J Transplant*. 2021;21:21-137.
19. Kieper WC, Jameson SC. Homeostatic expansion and phenotypic conversion of naïve T cells in response to self peptide/MHC ligands. *Proc Natl Acad Sci USA*. 1999;96:13306-13311.
20. Neujahr DC, Chen C, Huang X, et al. Accelerated memory cell homeostasis during T cell depletion and approaches to overcome it. *J Immunol*. 2006;176:4632-4639.
21. Pearl JP, Parris J, Hale DA, et al. Immunocompetent T-cells with a memory-like phenotype are the dominant cell type following antibody-mediated T-cell depletion. *Am J Transplant*. 2005;5:465-474.
22. Knechtle SJ, Pirsch JD, Fechner JH, et al. Campath-1H induction plus rapamycin monotherapy for renal transplantation: Results of a pilot study. *Am J Transplant*. 2003;3:722-730.
23. Flechner SM, Friend PJ, Brockmann J, et al. Alemtuzumab induction and sirolimus plus mycophenolate mofetil maintenance for CNI and steroid-free kidney transplant immunosuppression. *Am J Transplant*. 2005;5:3009-3014.

24. Noël C, Abramowicz D, Durand D, et al. Daclizumab versus antithymocyte globulin in high-immunological-risk renal transplant recipients. *J Am Soc Nephrol*. 2009;20:1385-1392.
25. Bamoulid J, Staeck O, Crépin T, et al. Anti-thymocyte globulins in kidney transplantation: Focus on current indications and long-term immunological side effects. *Nephrol Dial Transplant*. 2017;32:1601-1608.
26. Hricik DE, Formica RN, Nickerson P, et al. Adverse outcomes of tacrolimus withdrawal in immune-quiescent kidney transplant recipients. *J Am Soc Nephrol*. 2015;26:3114-3122.
27. Mohammed MT, Sage PT. Follicular T-cell regulation of alloantibody formation. *Curr Opin Organ Transplant*. 2020;25:22-26.
28. Macedo C, Hadi K, Walters J, et al. Impact of induction therapy on circulating T follicular helper cells and subsequent donor-specific antibody formation after kidney transplant. *Kidney Int Rep*. 2019;4:455-469.
29. Zhang R. Donor-specific antibodies in kidney transplant recipients. *Clin J Am Soc Nephrol*. 2018;13:182-192.
30. Wiebe C, Nickerson P. Posttransplant monitoring of de novo human leukocyte antigen donor-specific antibodies in kidney transplantation. *Curr Opin Organ Transplant*. 2013;18:470-477.
31. Hatzi K, Philip Nance J, Kroenke MA, et al. BCL6 orchestrates Tfh cell differentiation via multiple distinct mechanisms. *J Exp Med*. 2015;212:539-553.
32. Eto D, Lao C, DiToro D, et al. IL-21 and IL-6 are critical for different aspects of B cell immunity and redundantly induce optimal follicular helper CD4 T cell (Tfh) differentiation. *PLoS One*. 2011;6:e17739.
33. Poholek AC, Hansen K, Hernandez SG, et al. In vivo regulation of Bcl6 and T follicular helper cell development. *J Immunol*. 2010;185:313-326.
34. Jones JL, Phuah C-L, Cox AL, et al. IL-21 drives secondary autoimmunity in patients with multiple sclerosis, following therapeutic lymphocyte depletion with alemtuzumab (Campath-1H). *J Clin Invest*. 2009;119:2052-2061.
35. Papillion A, Powell MD, Chisolm DA, et al. Inhibition of IL-2 responsiveness by IL-6 is required for the generation of GC-TFH cells. *Sci Immunol*. 2019;4:eaaw7636.
36. Jogdand GM, Mohanty S, Devadas S. Regulators of Tfh cell differentiation. *Front Immunol*. 2016;7:1-14.
37. Crotty S. Follicular helper CD4 T cells (TFH). *Annu Rev Immunol*. 2011;29:621-663.
38. Ballesteros-Tato A, León B, Graf B, et al. Interleukin-2 inhibits germinal center formation by limiting T follicular helper cell differentiation. *Immunity*. 2012;36:847-856.
39. Ross SH, Cantrell DA. Signaling and function of interleukin-2 in T lymphocytes. *Annu Rev Immunol*. 2018;36:411-433.
40. Hirai T, Ramos TL, Lin P-Y, et al. Selective expansion of regulatory T cells using an orthogonal IL-2/IL-2 receptor system facilitates transplantation tolerance. *J Clin Invest*. 2021;131:e139991.
41. Liu R, Zhou Q, La Cava A, Campagnolo DI, Van Kaer L, Shi F-D. Expansion of regulatory T cells via IL-2/anti-IL-2 mAb complexes suppresses experimental myasthenia. *Eur J Immunol*. 2010;40:1577-1589.
42. Chung DT, Korn T, Richard J, et al. Anti-thymocyte globulin (ATG) prevents autoimmune encephalomyelitis by expanding myelin antigen-specific Foxp3+ regulatory T cells. *Int Immunol*. 2007;19:1003-1010.
43. Brennan DC, Daller JA, Lake KD, Cibrik D, Del Castillo D. Rabbit antithymocyte globulin versus basiliximab in renal transplantation. *N Engl J Med*. 2006;355:1967-1977.

SUPPORTING INFORMATION

Additional supporting information may be found in the online version of the article at the publisher's website.

How to cite this article: Gassen RB, Borges TJ, Pérez-Sáez MJ, et al. T cell depletion increases humoral response by favoring T follicular helper cells expansion. *Am J Transplant*. 2022;22:1766–1778. doi:10.1111/ajt.17038